

# Adaptive RBF -SMC control for multi-point mooring system

Run Lu<sup>\*</sup>, Guichen Zhang, and Jianqiang Shi

Merchant Marine College, Shanghai Maritime University, 1550 Haigang Ave, Shanghai 201306, P. R. China

**Abstract.** A stable adaptive control scheme for multi-point mooring system (MPMS) with uncertain dynamics is proposed in this paper. The control scheme is designed by a hybrid controller based on RBF (Radial Basis Function) NN (Neural Network) and SMC (Sliding Mode Control), which learns the MPMS dynamic changes, and the compensation of external disturbances is realized through adaptive RBFNN control. Meanwhile the RBF-SMC control parameters are adapted by the Lyapunov method to minimize squares dynamic positioning (DP) error. The convergence of the hybrid controller is proved theoretically, and the proposed mooring control scheme is applied to the “Kantan3” mooring simulation system. Finally, the simulation results are compared with the traditional PID controller and standard RBF controller to demonstrate the effective mooring positioning performance of the control scheme for the MPMS.

**Keywords:** Multi-point mooring, Dynamic positioning, SMC, RBF.

## 1 Introduction

Many kinds of offshore structures, such as mooring positioning system (MPMS), dynamic positioning (DP) system, and anchor auxiliary dynamic positioning system are being widely used in semi-submersible production platform. Among these platforms, the mooring system is characterized by less investment and convenience with maintenance; it is the main positioning system [1]. The mooring system provides the positioning restoring force for the semi-submersible platform by coordinating the mooring cable's retracting and releasing to generate resistance to environmental disturbance. At present, the research of deepwater mooring systems is mainly reflected in the dynamic analysis and the study of mooring damping. [2] considered the influence of nonlinear factors such as inertia, damping, and elastic deformation of anchor cable, the concentrated mass method is extended from the frequency domain to the time domain. [3] employed the time domain method to numerically analyze the dynamic effects of nonlinear coupling and uncoupling between the Spar platform's main body and the mooring system. For the design of the mooring system, the experimental results show that dynamic analysis is particularly

---

\* Corresponding author: [lurun2018@163.com](mailto:lurun2018@163.com)

important. [4] proposed a finite element technique for simulation of grounded and floating systems in the time domain, which assumed that the additional mass coefficient did not change significantly with frequency, and explained the dynamic characteristics of anchor chain reasonably.

A lot of research has been performed on the architecture of the DP control system relative to mooring control [5]. The initial DP control system added a low-pass filter to the traditional PID control model; nevertheless, the positioning accuracy of the controller is affected. To solve this problem, [6] proposed an approach that integrates optimal control with the principle of Kalman filters, and the actual scale was verified later by [7]. This recommendation has been amended, as presented in [8], which suppressed the high-frequency interference pulse but made the positioning error phase lag. [9] performed LQG control, which effectively eliminates high-frequency disturbance signals and reduces energy consumption, however, it has poor adaptability to the uncertainties of offshore platforms.

Robustness is the significant issue of the controller design because the vessel is suffered from wind, currents and waves in an extremely environment. Some scholars, including [10]-[11] applied the  $H^\infty$  control theory to prove that the controller has good robustness under great changes in environmental conditions. However, it is a linear controller based on a linear model. The multi-point mooring positioning process is an extremely nonlinear dynamics and oscillator. To solve its nonlinear problems, some methods have been applied to the DP.

## 2 Mathematical modeling of multi-point mooring system

### 2.1 Kinematics

A Cartesian coordinate system describes the motion of the multi-point mooring platform in Fig. 1. The basic coordinate system can be divided into the Earth-fixed  $X_E Y_E Z_E$  coordinate system and body-fixed coordinate system, the body frame is usually chosen at the platform's center of gravity conveniently.

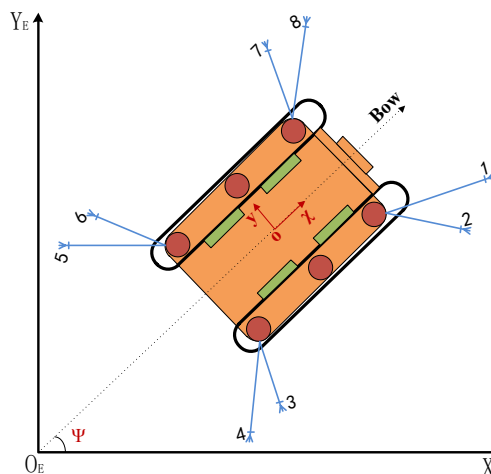


**Fig.1.** Reference coordinates of the platform.

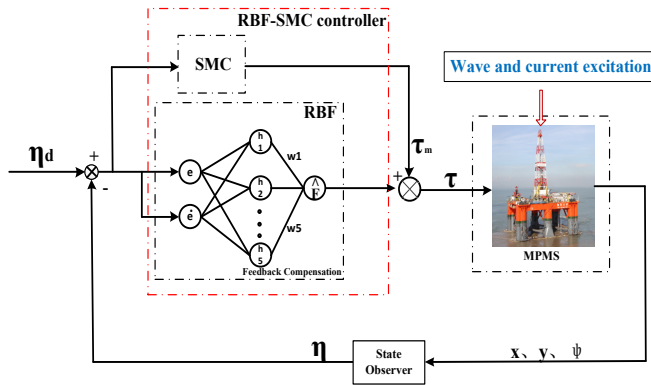


**Fig. 2.** The schematic of the multi-point mooring controller with RBF-SMC controller.

The elements of heave, roll and pitch motion causes the oscillation near the datum position of the platform, the elements of the surge, sway and yaw are the dominant motions to make the platform deviate from the datum position. Therefore, vectors  $\eta = [x \ y \ \psi]^T$  and  $v = [u \ v \ r]^T$  are defined to represent the position and bow angle of the working platform in the  $X_E Y_E Z_E$  coordinate system, yaw and bow velocity in the XYZ coordinate system respectively. The transformation relationship between  $\eta$  and  $v$  is as follows:

$$\dot{\eta} = J(\eta)v \tag{1}$$

The transformation matrix  $J(\eta)$  reduces to  $J(\psi)$  given by:

$$J(\eta) = J(\psi) = \begin{bmatrix} \cos\psi & -\sin\psi & 0 \\ \sin\psi & \cos\psi & 0 \\ 0 & 0 & 1 \end{bmatrix} \tag{2}$$

### 2.2 Nonlinear low-frequency model

The nonlinear coupling low-frequency motion equation of the multi-point mooring platform with anchoring automatic positioning in the direction of the surge, sway, and yaw in the moving coordinate system can be described as:

$$M \dot{v} + C(v)v + Dv = \tau_m + \tau_e \tag{3}$$

where  $M$  is the superposition of the additional mass matrix and inertia matrix,  $C(v)$  is the oblique symmetric Coriolis centripetal force matrix,  $D$  is the damping matrix, and  $\tau_m = [\tau_{mu} \ \tau_{mv} \ \tau_{mr}]^T$  is the generalized mooring control force and control moment vector produced by mooring cable.  $\tau_e = [\tau_{eu} \ \tau_{ev} \ \tau_{er}]^T$  represents the environmental forces (moments) exerted by wind, waves and ocean currents. It is possible to find descriptions of these terms in [12].

The matrixes  $M$ ,  $C(v)$  and  $D$  are given by:

$$M = \begin{bmatrix} m+m_x & 0 & 0 \\ 0 & m+m_y & 0 \\ 0 & 0 & I_z + I_{zz} \end{bmatrix} \quad C(v) = \begin{bmatrix} 0 & 0 & -m_v v \\ 0 & 0 & m_u u \\ m_v v & -m_u u & 0 \end{bmatrix} \quad D = \begin{bmatrix} -X_u & 0 & 0 \\ 0 & -Y_v & -Y_r \\ 0 & -N_v & -N_r \end{bmatrix}$$

### 3 RBF-SMC controller design

A MPMS consisting of multiple sensors information fusion, hybrid algorithms and many mooring winches. The sensors can detect the floating platform location and the mooring cable strain; the control algorithm calculates the force exerted on each mooring cable to counteract the environmental force. A simplified block diagram of a MPMS shown in Fig.2.

Considering Eqn. (1) and (3), the following equilibrium equation is given by

$$MJ^{-1}(\psi)\ddot{\eta} + (MJ^{-1}(\psi) + C(v)J^{-1}(\psi) + DJ^{-1}(\psi))\dot{\eta} = \tau_m + \tau_e \tag{4}$$

To simplify Eqn. (4), the definition is as follows

$$P(\eta) = MJ^{-1}(\psi) \tag{5}$$

$$Q(\eta, \dot{\eta}) = MJ^{-1}(\psi) + C(v)J^{-1}(\psi) \tag{6}$$

$$F(\eta, \dot{\eta}) = Dv - \tau_e \tag{7}$$

where  $|\tau_e| \leq \tau_{e\max}$ ,  $\tau_{e\max} > 0$

The formula obtained from Eqn. (4), (5), (6) and (7) is as follows

$$P(\eta)\ddot{\eta} + Q(\eta, \dot{\eta})\dot{\eta} + F(\eta, \dot{\eta}) = \tau_m \tag{8}$$

Eqn. (8) is simplified by 3-DOF as follows

$$\ddot{\eta} = -P^{-1}Q\dot{\eta} - P^{-1}F + P^{-1}\tau_m \tag{9}$$

The sliding surface can be defined as:

$$s = \kappa e + \dot{e} \tag{10}$$

where  $\kappa > 0$ ,  $e$  and  $\dot{e}$  is the position error and derivative of the error, respectively. It

should be noted that  $e = [e_x \quad e_y \quad e_\psi]^T$  consists of the position error in the surge, sway, and yaw detections, respectively.

$$e = \eta_d - \eta \tag{11}$$

$$\dot{e} = \dot{\eta}_d - \dot{\eta} \tag{12}$$

Take the derivative concerning S is given by

$$\dot{s} = \kappa\dot{e} + \ddot{\eta}_d - P^{-1}\tau_m + P^{-1}F + P^{-1}Q\dot{\eta} \tag{13}$$

The SMC control law is given by:

$$\tau_m = \kappa P\dot{e} + P\ddot{\eta}_d + F + Q\dot{\eta} + \varepsilon P \operatorname{sgn}(s) + \lambda Ps \tag{14}$$

To reduce vibration problems, the saturation function  $\operatorname{sat}(s)$  is adopted to supersede the sign function  $\operatorname{sgn}(s)$  in the controller.

$$sat(s) = \begin{cases} \frac{s}{\Delta} & |s| \leq \Delta \\ \text{sgn}(s) & |s| > \Delta \end{cases} \quad (15)$$

where  $\Delta$  is the boundary layer.

The three-layer feedforward network of the RBF with good performance and the NN is adopted in this paper to approximate the uncertain function  $F(\eta, \dot{\eta})$ , and the network algorithm is as follows:

$$F(\sigma) = W^{*T}h(\sigma) + \delta \quad (16)$$

Take the Gaussian  $h(\sigma)$  as follows:

$$h_j = \exp\left(-\frac{\|\sigma - c_j\|^2}{2b_j^2}\right) \quad (17)$$

where  $j$  is the NN hidden layer node,  $j=1, 2, 3, \dots, n$ ;  $\sigma$  is a vector of input layer for the network;  $\|\cdot\|$  denotes the Euclidean norm;  $c_j$  is a vector of center;  $b_j$  is the Gaussian extension width;  $W^*$  is the ideal weight of the NN;  $\delta$  is the approximation error of the NN. For simplicity, the centers and widths are pre-defined and fixed. In this paper, the input layer  $\sigma$  and NN output  $\hat{F}(\sigma)$  can be expressed as:

$$\sigma = \begin{bmatrix} e & \dot{e} \end{bmatrix}^T \quad (18)$$

$$\hat{F}(\sigma) = \hat{W}^T h(\sigma) \quad (19)$$

RBF NN is utilized to approximate the unknown term  $F$  in Eqn.(14), and the final RBF-SMC control law is designed as:

$$\tau = \kappa P\dot{e} + P\ddot{\eta}_d + \hat{F} + Q\dot{\eta} + \varepsilon P sat(s) + \lambda Ps \quad (20)$$

Eqn. (20) is substituted by Eqn. (13) as follows

$$\dot{s} = \tilde{F} - \varepsilon sat(s) - \lambda s \quad (21)$$

where

$$\tilde{F} = \hat{F} - F = \hat{W}^T h(\sigma) - W^{*T} h(\sigma) - \delta = -\tilde{W}h(\sigma) - \delta \quad (22)$$

$$\hat{W} = W^* - \tilde{W} \quad (23)$$

The corresponding adaptive law is designed as follows:

$$\dot{\hat{W}} = -\frac{1}{\gamma} sh(\sigma) \quad (24)$$

where  $\hat{W}$  is the estimation of  $W^*$  and  $\gamma$  is a positive constant.

The Lyapunov function defined as:

$$L = \frac{1}{2}s^2 + \frac{1}{2}\gamma\tilde{W}^T\tilde{W} \quad (25)$$

The derivative of the Lyapunov function is given by

$$\begin{aligned} \dot{L} &= s\dot{s} + \gamma\tilde{W}^T\dot{\tilde{W}} = s(\tilde{F} - \varepsilon\text{sat}(s) - \lambda s) - \gamma\tilde{W}^T\dot{\tilde{W}} \\ &= s(-\tilde{W}^T h(\sigma) - \delta - \varepsilon\text{sat}(s) - \lambda s) - \gamma\tilde{W}^T\dot{\tilde{W}} \\ &= -\tilde{W}^T (sh(\sigma) + \gamma\dot{\tilde{W}}) - s(\delta + \varepsilon\text{sat}(s) + \lambda s) \end{aligned} \quad (26)$$

Eqn. (26) is substituted by Eqn. (24) as follows

$$\dot{L} = -s(\delta + \varepsilon\text{sat}(s) + \lambda s) = -s(\delta + \varepsilon\text{sat}(s)) - \lambda s^2 \quad (27)$$

The RBF approximation error  $\delta$  is a very small positive number,  $\varepsilon > \delta$ .

$$\dot{L} \leq -s(\delta + \varepsilon\text{sat}(s)) \quad (28)$$

There are  $\dot{L} \leq 0$ ,  $\dot{L} \equiv 0$  and  $s \equiv 0$ . Based on the principle of LaSalle invariant set,  $t \rightarrow \infty$  and  $s \rightarrow 0$ , the multi-point mooring DP system is asymptotically stable. Above all, it can be show that the designed sliding mode surface gradually converges to the origin, the consistency and ultimate boundedness of the error signal are ensured.

## 4 Results and analysis

In order to verify the effects of the RBF-SMC controller, the semi-submersible offshore platform “Kantan3” is the research object and simulated. Table 2 gives the key dimensions and mass characteristics of the platform under operating conditions. According to the calculation formula (Fossen, 2011), the mass matrix and damping matrix of the platform can be written as:

$$M = \begin{bmatrix} 5.43 \times 10^6 & 0 & 0 \\ 0 & 8.32 \times 10^6 & 0 \\ 0 & 0 & 9.02 \times 10^9 \end{bmatrix} \quad D = \begin{bmatrix} 5.24 \times 10^4 & 0 & 0 \\ 0 & 4.71 \times 10^4 & -1.12 \times 10^6 \\ 0 & -1.12 \times 10^6 & 1.02 \times 10^8 \end{bmatrix}$$

**Table 1.** “Kantan3” semi-submersible platform information.

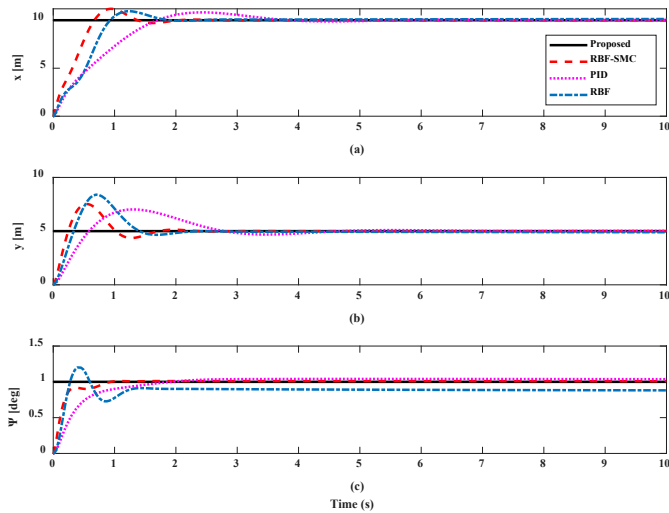
Parameter	Unit	Value
Length(L)	m	91
Beam(B)	m	71
Draft(T)	m	20.0
Z COG (to baseline)	m	15.75
Displacement(D)	Ton	25240
Roll radius of gyration	m	26.52
Pitch radius of gyration	m	29.97
Yaw radius of gyration	m	33.90

### 4.1 Setting-point control test

The setting point control tested the RBF-SMC controller's ability of location accuracy of calibration points. Expected platform position  $\eta_d = [10m \ 5m \ 1rad]^T$ , the initial position  $\eta_0 = [0m \ 0m \ 0rad]^T$ .

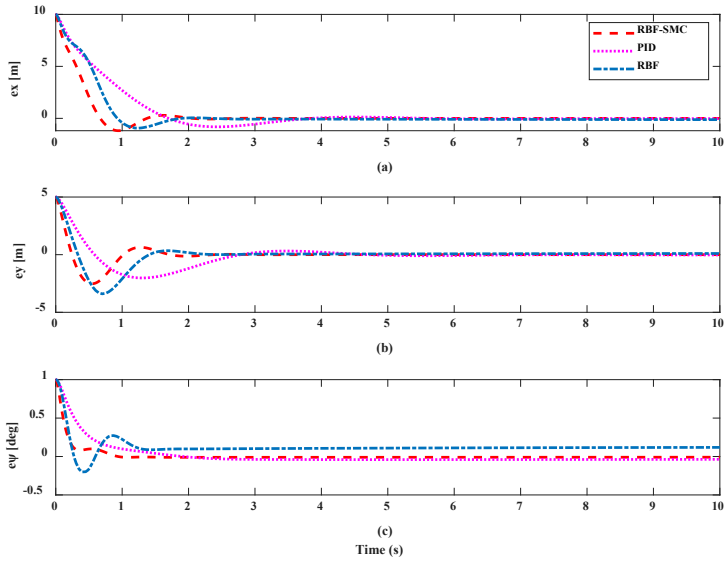
The setting point position tracking curve of surge, sway and yaw motion is shown in Fig. 3. Simulation results show that, compared with traditional PID control and RBF control, RBF-SMC control can significantly reduce the maximum overshoot time and rise time, suppress oscillation and finally converge to a given point. Fig. 4 is a setting point position tracking error curve of surge, sway and yaw motion. Compared with the other two controllers, the positioning error value of RBF-SMC control keeps the minimum, and the error is basically zero after reaching stability. In the yaw direction, the positioning error always exists because of the boundary value limitation in the NN controller.

Fig. 5 shows the velocity variation curves of the three control modes in setting point control, Fig. 6 shows the setting point position tracking movement route of the mooring platform in the earth coordinate system. From the curve changes, it can be seen that the response speed of RBF-SMC control is faster than the other two controls, and it has the best movement path.



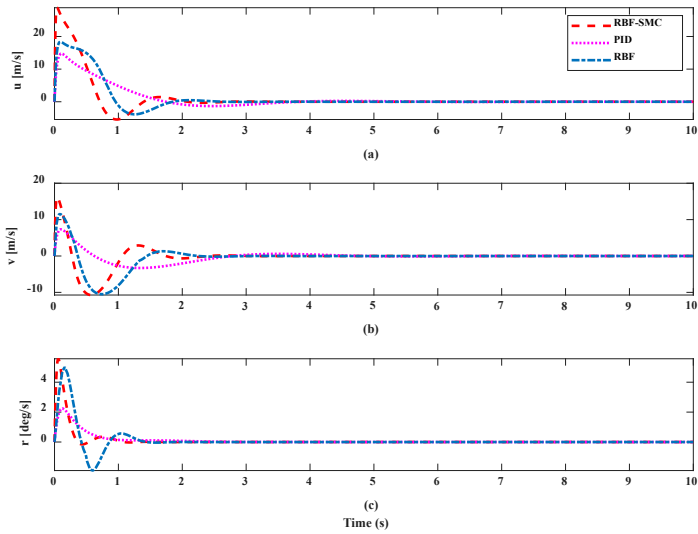
(a) surge direction; (b) sway direction; (c) yaw direction

**Fig. 3.** Position tracking of RBF-SMC controller for setting point.



(a) surge direction; (b) sway direction; (c) yaw direction

**Fig. 4.** Position tracking error of RBF-SMC controller for setting point.



(a)surge direction; (b)sway direction; (c) yaw direction.

**Fig. 5.** Velocity tracking of RBF-SMC controller for setting point.

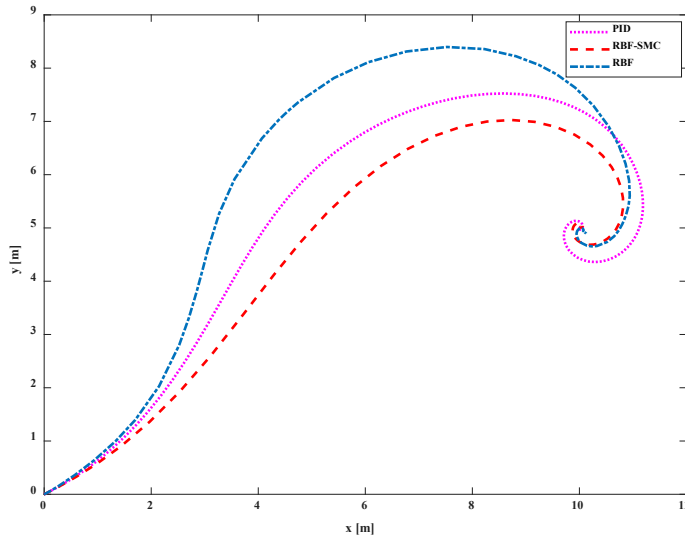


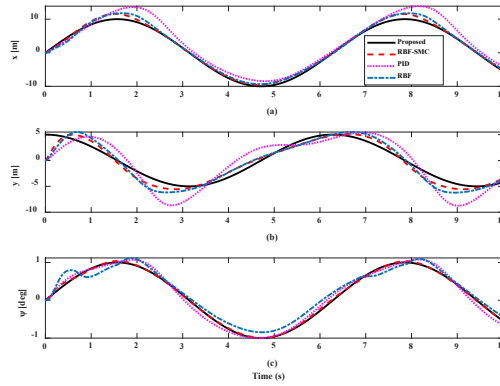
**Fig. 6.** The setting point control of platform position in the XY plane.

## 4.2 Trajectory tracking control test

The sinusoidal trajectory tracking process of the semi-submersible offshore mooring platform positioning is simulated; its parameters are the same as setting point control. The simulation time is 10 seconds and the expected trajectory is changed as follows:

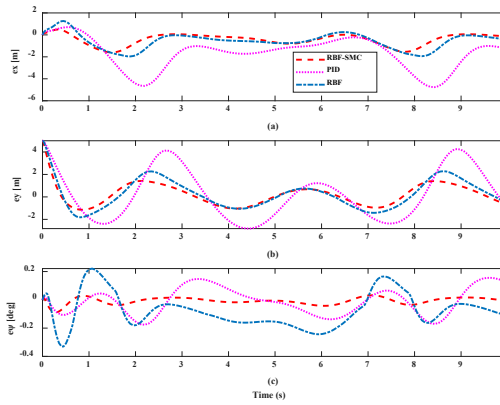
$$\eta_d = \begin{bmatrix} 10 \sin t \\ 5 \cos t \\ \sin t \end{bmatrix}$$

In the sinusoidal trajectory tracking control, the trajectory position tracking curves of surge, sway and yaw motions are shown in Fig. 8. The rising amplitude of horizontal displacement of PID control and RBF control is larger than that of RBF-SMC control. The maximum offset of horizontal movement of mooring platform with RBF-SMC controller is suppressed, and the dynamic positioning accuracy is higher. The error curve of sinusoidal track position tracking is shown in Fig. 9. The traditional PID control always has a large position tracking error. The position tracking error of RBF control is obvious in yaw motion, and the position tracking error of RBF-SMC control tends to zero after reaching stability. It shows that RBF-SMC controller has better adaptability and robustness under irregular wave conditions.



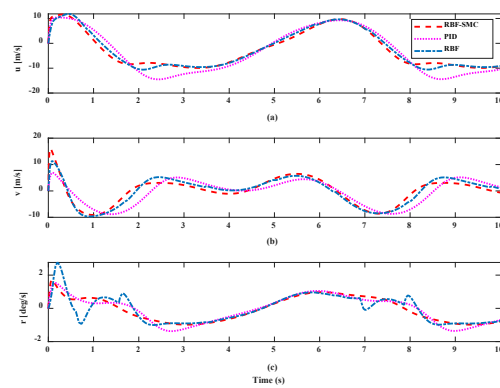
(a) surge direction; (b) sway direction; (c) yaw direction.

**Fig. 8.** Position tracking of RBF-SMC controller.



(a) surge direction; (b) sway direction; (c) yaw direction.

**Fig. 9.** Position tracking error of RBF-SMC controller.



(a) surge direction; (b) sway direction; (c) yaw direction.

**Fig. 10.** Velocity tracking of RBF-SMC controller.

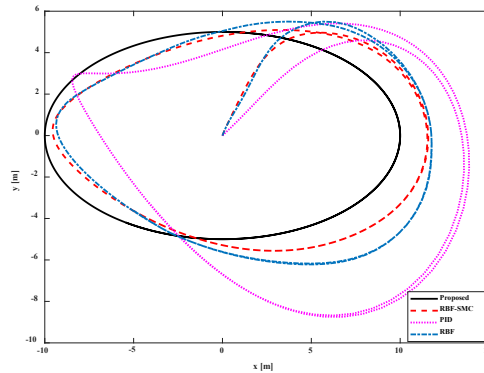


**Fig. 11.** The trajectory tracking control of platform position in the XY plane.

Fig. 10 is a speed variation curve of surge, sway and yaw in sinusoidal trajectory tracking control. Affected by wind, waves and currents, the mooring platform swings along the rocking direction, and the speed of the mooring platform is smoother in the positioning process by adopting RBF-SMC controller. The position tracking effect of the mooring platform in the earth coordinate system is shown in Fig. 11. The maximum values of PID control and SMC control are 4.6 m and 2.1 m; respectively. The RBF-SMC control is used to reduce the position deviation to 1.2 m.

## 5 Conclusions

In this paper, a stable adaptive control scheme for MPMS with uncertain dynamics is proposed. The control scheme is designed by a hybrid controller based on RBF NN and SMC, which learns the MPMS dynamic changes, and the compensation of external disturbances is realized through adaptive RBFNN control. The proposed mooring control scheme is applied to the “Kantan3” mooring simulation system. Firstly, the setting point position tracking control experiment is carried out under the condition of irregular waves, and then the sinusoidal trajectory tracking control experiment is carried out. Comparing the simulation results with standard PID controller and traditional RBF controller, the following conclusions are drawn.

1) Compared with PID controller and RBF controller, RBF-SMC controller can significantly reduce the maximum overshoot time and rise time, suppress oscillation and finally converge to a given point. With the movement of the setting point, RBF-SMC controller has better stability and robustness under irregular wave conditions.

2) The RBF-SMC controller is adaptive to the evolution conditions, and can approach the uncertainty of the model dynamically, thus reducing the fuzzy advantage under the disturbance of variable environment. On the horizontal axis, the positioning accuracy is greatly improved.

This project is supported by the National Natural Science Foundation of China (Grant No.51779136).

## References

1. Zhou, S. L., Nie, W., & Bai, Y. (2010). Investigation on mooring system design of a deepwater semi-submersible platform. *Journal of Ship Mechanics*. 14(5), 495–502.

2. Koterayama, W., & Nakamura, M. (1992). Drag and inertia force coefficients derived from field tests. *International Journal of Offshore and Polar Engineering*, 2(3), 161-167.
3. Kim, M. H., Ran, Z. H., & Zheng, W. H. (2001). Hull/mooring coupled dynamic analysis of a truss spar in the time domain. *International Journal of Offshore and Polar Engineering*, 11(1), 42-54.
4. Nakamura, M., Koterayama, W., & Kyojuka, Y. (1991). Slow drift damping due to drag forces acting on mooring lines. *Ocean Engineering*, 18(4), 283-296.
5. Xu, S., Wang, X., Yang, J., & Wang, L. (2019). A fuzzy rule based PID controller for dynamic positioning of vessels in variable environmental disturbances. *Journal of Marine Science and Technology* 25(3), 914-924.
6. Balchen, J. G., Jenssen, N. A., & Saelid, S. (1976). Dynamic positioning using Kalman filtering and optimal control theory. In *IFAC/IFIP Symposium on Automation in Offshore Oil Field Operation* (pp. 183-186), The Netherlands.
7. Balchen, J. G., Jenssen, N. A., & Saelid, S. (1980). Dynamic positioning of floating vessels based on Kalman filtering and optimal control. In *Proceedings of the 19th IEEE Conference on Decision and Control* (pp. 852-864), USA.
8. Saelid, S., Jenssen, N. A., & Balchen, J. G. (1983). Design and analysis of a dynamic positioning system based on Kalman filtering and optimal control., *IEEE Transactions on Automatic Control*, 28(3), 331-339.
9. Javling, B., Balchen, J. G., & Strand, S. (1993). Modified LQG-control and quasi-dynamic optimal control for nonlinear multivariable processes. *IFAC Proceedings Volumes*, 26(2), 89-92.
10. Katebi, M. R., Rible, M. J. G., & Zhang, Y. (1997).  $H_{\infty}$  robust control design for dynamic ship positioning. *IEEE Proceedings Control Theory and Applications*, 144(2), 110-120.
11. Hyakudome, T., Nakamura, M., Kajiwara, H., & Kotemiyama, W. (1998).  $H_{\infty}$  Control of Slow Drift Oscillation of Moored Floating Platform with Thrusters. *The Proceedings of the Eighth (1998) International Offshore and Polar Engineering Conference* (pp. 338-345), Japan.
12. Fossen, T. I. (2011). *Handbook of Marine Craft Hydrodynamics and Motion Control*, John Wiley and Sons Published.